



Minerva Access is the Institutional Repository of The University of Melbourne

**Author/s:**

Micati, DJ;Hime, GR;McLaughlin, EA;Abud, HE;Loveland, KL

**Title:**

Differential expression profiles of conserved Snail transcription factors in the mouse testis

**Date:**

2018-03-01

**Citation:**

Micati, D. J., Hime, G. R., McLaughlin, E. A., Abud, H. E. & Loveland, K. L. (2018). Differential expression profiles of conserved Snail transcription factors in the mouse testis. *Andrology*, 6 (2), pp.362-373. <https://doi.org/10.1111/andr.12465>.

**Persistent Link:**

<https://hdl.handle.net/11343/283540>

1  
2  
3  
4  
5  
6  
7  
8  
9  
10  
11  
12  
13  
14  
15  
16  
17  
18  
19  
20  
21  
22  
23  
24  
25  
26  
27

MISS DIANA MICATI (Orcid ID : 0000-0003-3503-9434)

Article type : Original Article

## **Differential expression profiles of conserved Snail transcription factors in the mouse testis**

Diana J Micati<sup>1,7</sup>, Gary R Hime<sup>2</sup>, Eileen A McLaughlin<sup>3,4</sup>, \*Helen E Abud<sup>5</sup>, and \*Kate L Loveland<sup>1,6,7</sup>

\*Helen E Abud and Kate L Loveland are senior co-authors

1. Department of Molecular and Translational Sciences, Monash University, Melbourne, Victoria, 3800, Australia
2. Department of Anatomy and Neuroscience, University of Melbourne, Melbourne, Australia
3. School of Environmental and Life Sciences, University of Newcastle, Callaghan, NSW, 2308, Australia
4. School of Biological Sciences, University of Auckland, Auckland, 1152, New Zealand
5. Cancer Program, Monash Biomedicine Discovery Institute and Department of Anatomy and Developmental Biology, Monash University, Victoria, 3800, Australia
6. Department of Anatomy and Developmental Biology, Monash University, Melbourne, Victoria, 3800, Australia
7. Centre for Reproductive Health, Hudson Institute of Medical Research, Melbourne, Victoria, 3168, Australia

Correspondence should be addressed to K.L.

Phone +61 3 8572 2904

This is the author manuscript accepted for publication and has undergone full peer review but has not been through the copyediting, typesetting, pagination and proofreading process, which may lead to differences between this version and the [Version of Record](#). Please cite this article as [doi: 10.1111/andr.12465](https://doi.org/10.1111/andr.12465)

This article is protected by copyright. All rights reserved

28 Address: Level 3, MHRP Building, Hudson Institute of Medical Research, 27-31 Wright  
29 Street, Clayton, 3168, Australia

30 Email: kate.loveland@monash.edu

31 Running title: Snail expression in mammalian testis

32 **Funding information:** Work was supported by grants from the National Health and Medical  
33 Research Council of Australia (Project grant ID1048110 to GH, HA, KL and Fellowship  
34 ID1079646 to KL).

35

36

37 **Abstract**

38

39 Snail transcription factors are key regulators of cellular transitions during embryonic  
40 development and tumorigenesis. The closely related SNAI1 and SNAI2 proteins induce  
41 epithelial-mesenchymal transitions (EMTs), acting predominantly as transcriptional  
42 repressors, while the functions of SNAI3 are unknown. An initial examination of *Snai2*-  
43 deficient mice provided evidence of deficient spermatogenesis. To address the hypothesis that  
44 Snail proteins are important for male fertility, this study provides the first comprehensive  
45 cellular expression profiles of all three mammalian Snail genes in the postnatal mouse testis.  
46 To evaluate Snail transcript expression profiles, droplet digital (dd) PCR and *in situ*  
47 hybridisation were employed. *Snai1*, 2, and 3 transcripts are readily detected at 7, 14, 28 days  
48 postpartum (dpp) and 7 weeks (adult). Unique cellular expression was demonstrated for each  
49 by *in situ* hybridisation and immunohistochemistry using Western blot-validated antibodies.  
50 SNAI1 and SNAI2 are in the nucleus of the most mature germ cell types at postnatal ages 10,  
51 15, and 26. SNAI3 is only detected from 15 dpp onwards, and is localised in the Sertoli cell  
52 cytoplasm. In the adult testis, *Snai1* and *Snai2* transcripts are detected in spermatogonia and  
53 spermatocytes, while *Snai3* is in both germ and Sertoli cells. SNAI1 protein is evident in  
54 nuclei of spermatogonia, spermatocytes, round spermatids, and elongated spermatids (Stages  
55 IX-XII). SNAI2 is present in the nuclei of spermatogonia and spermatocytes, with a faint  
56 signal detected in round spermatids. SNAI3 was detected only in Sertoli cell cytoplasm, as in  
57 the juvenile testes. Additionally, co-localisation of SNAI1 and SNAI2 with previously

58 identified key binding partners, LSD1 and PRC2 complex components, provides strong  
59 evidence that these important functional interactions are conserved during spermatogenesis to  
60 control gene activity. These distinct expression profiles suggest that each Snail family  
61 member has unique functions during spermatogenesis.

62

63

#### 64 **Keywords**

65 Snail transcription factors – Postnatal mouse testis - Germ cells – Spermatogenesis - Cycle of  
66 the seminiferous epithelium

67

#### 68 **Introduction**

69 Spermatogenesis is characterized by a series of essential cellular transitions that are required  
70 for the production of functional spermatozoa. Each spermatogenic stage involves changes in  
71 gene expression that are tightly regulated, and this study addresses the hypothesis that Snail  
72 transcription factors contribute to the correct progression of germline development.

73 Snail proteins belong to a large superfamily of zinc-finger transcription factors that play  
74 crucial roles in transcriptional regulation, cellular migration, chromatin remodelling, cell  
75 signalling and impact on many developmental processes (Batlle, Sancho et al. 2000, Kalluri  
76 and Weinberg 2009, Lin, Dong et al. 2014), including mesoderm formation and neural crest  
77 cell migration during embryogenesis (Alberga, Boulay et al. 1991). Additionally, Snail  
78 family members are overexpressed in various cancers where they are major regulators of cell  
79 survival, proliferation, and invasion (Turner, Broad et al. 2006, Uygur and Wu 2011).

80 The mammalian Snail family has three members, SNAI1, SNAI2, and SNAI3. Each features  
81 a highly conserved carboxy- (C) terminal region and a more divergent amino (N) terminal  
82 region, particularly for SNAI3 (Kataoka, Murayama et al. 2000, Nieto 2002). A conserved  
83 DNA-binding domain within the C-terminus contains four to six zinc fingers which directly  
84 interact with target genes to regulate their activity. The N-terminal region is composed of the  
85 SNAG transactivation domain, which interacts both directly and indirectly with co-factor  
86 proteins to form multi-molecular structures that drive target gene repression (Chiang and  
87 Ayyanathan 2013). Snail co-factors are chromatin remodelling enzymes. These include:

88 LSD1, HDAC1/2, EZH2, G9a and SUV39H1 (Lin, Dong et al. 2014), and several of these  
89 have critical roles in the reprogramming of the transcriptome during spermatogenesis,  
90 promoting both spermatogonial differentiation (Myrick, Christopher et al. 2017), and  
91 progression of meiosis (Mu, Starmer et al. 2014).

92 Spermatogenesis is a complex process by which mature spermatozoa are produced through a  
93 series of cellular divisions and maturation steps, each featuring a unique transcriptome  
94 (Ahmed and de Rooij 2009, Shalet 2009). Germ cells are strictly organised within the  
95 seminiferous epithelium formed by Sertoli cells, so that each generation of spermatogonia,  
96 spermatocytes and spermatids develops in parallel with subsequent generations, in a highly  
97 ordered, cyclic manner, termed Stages (Leblond and Clermont 1952). The cycle of the  
98 seminiferous epithelium of the adult mouse testis is considered as divided into 12 Stages (I-  
99 XII) (Oakberg 1956, Hess and Renato de Franca 2008). In mice, the first complete cycle of  
100 spermatogenesis commences at 7 days post-partum (dpp) and yields spermatozoa by 42 dpp. .  
101 Key time points corresponding to the first appearance of a particular germ cell type have been  
102 identified during the first wave of spermatogenesis. At 7 dpp, the mouse seminiferous cords  
103 contain only Sertoli cells and spermatogonia. At 14 dpp, spermatocytes are present within the  
104 tubules which form when post-mitotic Sertoli cells secrete fluids in an apical directions. As a  
105 result of meiotic divisions, round spermatids are first formed at 28 dpp. These haploid cells  
106 undergo morphological changes to first produce elongated spermatids at 30 dpp, and  
107 functional spermatozoa by 35 dpp (Fig. 1 a) (Kramer and Erickson 1981). The transition from  
108 one spermatogenic cell type to the next is governed by tight control of transcription (Eddy  
109 1998). This progressive emergence of each more mature germ cell type during the first wave  
110 of spermatogenesis in juveniles provides a good opportunity to visualise how the dynamic  
111 changes in gene expression are coordinated by transcriptional regulators.

112 The *Snai*-deficient mice for which a testicular phenotype has been reported are those lacking  
113 *Snai2* which exhibit pigmentation, epithelial and hematopoietic defects (Cobaleda, Perez-  
114 Caro et al. 2007). The testis was only analysed in these *Snai2* deficient mice at six week of  
115 age; they display testicular atrophy, resulting from an apparent reduction in germ cell number  
116 (Perez-Losada, Sanchez-Martin et al. 2002), although this has not been quantitated. In  
117 addition, *Snai2* knockout mice are reported to be subfertile. Fertility was analysed in other  
118 *Snai*-deficient mouse models. Specifically, the complete absence of *Snai3* does not affect the  
119 testicular phenotype (Bradley, Norton et al. 2013), implying that SNAI3 is not necessary for  
120 spermatogenesis. However mice lacking both *Snai2* and *Snai3* have been reported to be

121 infertile (Pioli, Dahlem et al. 2013), suggesting that SNAI2 and SNAI3 are functionally  
122 redundant in the testis. This result is surprising given the structural differences between  
123 SNAI2 and SNAI3; this potential has not been investigated further. A different study,  
124 examining ubiquitin ligase  $\beta$ -TrCP knockout mice, provided indirect evidence that elevated  
125 SNAI1 levels can impair spermatogenesis. In this strain, the prominent nuclear SNAI1  
126 immunostaining in spermatogonia suggested that SNAI1 was not targeted for proteasomal  
127 degradation and resulted in spermatogonial cell loss (Kanarek, Horwitz et al. 2010).  
128 However, analysis of the testes in both of these mouse models was limited. In the present  
129 study, ddPCR, *in situ* hybridisation and immunohistochemistry are used to document the  
130 cellular expression profiles of all three Snail family members in the normal postnatal mouse  
131 testis, including during pre- and post-pubertal development. The findings reveal distinct  
132 cellular expression profiles for the Snail mRNAs and proteins that are concordant with  
133 developmental switches during cellular differentiation. Importantly, we provide evidence that  
134 these co-localise with previously identified Snail co-factors, thereby providing a platform for  
135 understanding the potential functions of Snail family members during the cellular transitions  
136 of spermatogenesis.

137

## 138 **Materials and Methods**

### 139 **Animal Ethics**

140 All procedures involving animal samples were approved by the Monash Animal Research  
141 Platform (MARP) Ethics Committee and conformed to the National Health and Medical  
142 Research Council (NHMRC) of Australia's Code of Practice for the Care and Use of Animals  
143 for Experimental Purposes.

144

### 145 **Mouse tissues and histological sections**

146 For histology, C57Bl/6J mice were obtained from (MARP). Testis sections at various ages  
147 including 10, 15, 26 days post-partum (dpp) and adult (60-90 dpp) were first fixed in Bouin's  
148 or 4% PFA for 3-5 hrs, then paraffin-embedded using the Shandon Histocentre 3 (Thermo  
149 Electron Corporation) at the Monash University Histology Facility. Sections of 5  $\mu$ m were  
150 dried onto Superfrost 2 glass slides (Menzel-Glaser, Braunschweig, Germany). *Snai2*  
151 knockout tissue was obtained from the *Snai2*<sup>LacZ</sup> mouse line, generated by replacing the zinc

152 finger coding region of the *Snai2* gene with the  $\beta$ -galactosidase gene (Jiang, Lan et al. 1998).  
153 PFA-fixed adult mouse testis samples (*Snai2*<sup>+/+</sup>, n=1; and *Snai2*<sup>-/-</sup>, n=1) were kindly  
154 provided by Professor Donna Frances Kusewitt (MD Anderson, Smithville, Texas) to verify  
155 the specificity of the SNAI2 antibody.

156

#### 157 *Droplet digital PCR*

158 Total RNA was extracted from four decapsulated Swiss mouse testes at postnatal days 7, 14,  
159 28 and adult (Week 7) using TRIzol reagent (Invitrogen, Thermo Fisher Scientific, Waltham,  
160 USA). Genomic DNA contamination was eliminated by DNase treatment using DNase-free  
161 kit (Ambion, Thermo Fisher Scientific, Waltham, USA). cDNA was synthesised using 100 U  
162 Superscript III reverse transcriptase (Invitrogen, Thermo Fisher Scientific, Waltham, USA)  
163 with 2.5  $\mu$ M random hexamer oligonucleotides (Roche, Basal, Switzerland). Methods were  
164 performed according to manufacturers' instructions. cDNA was diluted 1:10 with filtered  
165 MilliQ water and quantified using the QIAxpert system (QIAGEN, Hilden, Germany).

166 The cDNAs from enriched preparations of spermatogonia (> 95% pure; n = 3),  
167 spermatocytes (> 85% pure; n = 3) and round spermatids (> 88% pure; n = 2) were used in  
168 previous studies and supplied at a 1:10 dilution for these experiments. Spermatogonia had  
169 been isolated from 8 days old mouse testes, while 8 week old mouse testes were used for  
170 isolation of spermatocytes and round spermatids. Samples were collected from a 2-4%  
171 continuous bovine serum albumin (BSA) gradient, as previously described (McIver, Stanger  
172 et al. 2012, Bromfield, Aitken et al. 2017).

173 Digital droplet (dd) PCR was performed using the BioRad QX100/200 system. The ddPCR  
174 reaction contained 12.5  $\mu$ l of 2 x ddPCR Supermix for probes (BioRad, Hercules, USA),  
175 1.25  $\mu$ l of 20 x target probes with a FAM dye label (final concentration 250 nM each), 2  $\mu$ l of  
176 1:10 template dilution, and filtered MilliQ water to a final volume of 25  $\mu$ l. Twenty  $\mu$ l of  
177 ddPCR reaction followed by 70  $\mu$ l of droplet generator oil for probes (BioRad, Hercules,  
178 USA) were loaded into a DG8<sup>TM</sup> cartridge for the QX100/200 droplet generator (BioRad,  
179 Hercules, USA). Droplets produced were transferred into a 96 well plate (Eppendorf,  
180 Hamburg, Germany) and a two-step thermocycling protocol [(enzyme activation at 95°C x 10  
181 mins); 40 cycles x (denaturation at 94°C x 30s, annealing at 59°C x 60s, enzyme deactivation  
182 at 98°C X 10 mins), ramp rate set at 2.5°C/s] was performed in a thermalcycler (BioRad  
183 C1000 Touch). The plate was then placed in a QX100/200 Droplet Reader (BioRad,

184 Hercules, USA). Data were analysed using the QuantaSoft analysis software (BioRad,  
185 Hercules, USA). Age series values and isolated germ cell data were not normalised. Data  
186 were reported as the means  $\pm$  standard error of the means (SEM).

187 Probes, supplied by IDT (Coralville, USA), were: *Snai1* (MmPT. 58.43057042); *Snai2*  
188 (MmPT. 58.5576027); *Snai3* (MmPT. 58.43894205).

189

#### 190 *DIG-labelled RNA probes and in situ hybridisation*

191 Primer sequences used to generate *in situ* hybridisation probes are listed in Table 1. The  
192 following PCR parameters were used to amplify target transcript regions: 95°C for 3 mins; 40  
193 cycles of 95°C (30s), 61°C (30s), 72°C (30s); 72°C for 7 mins using 1  $\mu$ l cDNA. Templates  
194 used were adult mouse testis (to amplify *Snai1* and *Snai3*) and 6 dpp (to amplify *Snai2*). PCR  
195 products were purified (QIAquick PCR Purification Kit, QIAGEN, Hilden, Germany), cloned  
196 in pGEM T-Easy vector (Promega, Madison, USA) following the manufacturer's guidelines  
197 and sequenced (Big Dye Terminator v3.1 Cycle Sequencing Kit, ABIPRISM 377 DNA  
198 Sequencer, Applied Biosystems) by the Gandel Charitable Trust Sequencing Centre, Hudson  
199 Institute of Medical Research, Clayton, VIC, Australia. PCR amplification of these plasmids  
200 using pBS forward and reverse primers produced products that included T7 and Sp6  
201 polymerase binding sites which were used as templates for *in vitro* transcription to generate  
202 antisense and sense cRNA probes (Itman, Wong et al. 2011).

203 *In situ* hybridisation was performed on Bouin's fixed, paraffin embedded, adult mouse testis  
204 sections to determine the cellular sites where *Snai1*, *Snai2* and *Snai3* transcripts are  
205 synthesised using standard procedures (Itman, Wong et al. 2011). Briefly, slides were  
206 dewaxed and rehydrated. To permeabilise the tissue, sections were incubated with Proteinase  
207 K solution (Roche, Basal, Switzerland) at 37°C for 30 mins. Tissue sections were incubated  
208 with Prehybridisation buffer (50% v/v DIF, 14% v/v 20 x SSC, 33% v/v phosphate buffer,  
209 4% v/v 50 x Denhardt's solution) for 2 hrs at 50 - 55°C in a hybridisation oven within a  
210 covered humid chamber. Hybridisation was performed with 150 ng/100  $\mu$ l probe per slide at  
211 50 - 55°C overnight, followed by washes of 15 mins from 2 x SSC to 0.1 x SSC at the  
212 hybridisation temperature. Bound DIG-labelled cRNA probes were detected by anti-DIG  
213 antibody (1:1000 dilution, Roche, Basal, Switzerland) and visualised by alkaline phosphatase  
214 developer (BCIP/NBT, Thermo Fisher Scientific, Waltham, USA). Slides were  
215 counterstained with Harris Hematoxylin (diluted 1:3 v/v) and mounted under coverslips in

216 GVA aqueous solution (Genemed Biotechnologies, South San Francisco, USA). In situ  
217 hybridisation was performed three times using adult testis sections from two different mice.  
218 Slides were imaged on a Zeiss imager A.1 microscope with an AxioCam MRc5.

219

## 220 *Immunohistochemistry*

221 Immunohistochemistry was performed as previously described (Dias, Rajpert-De Meyts et al.  
222 2009). Immunostaining with anti-SNAI1, anti-SNAI2, anti-EED, anti-EZH2, and anti-LSD1  
223 was performed on PFA-fixed testis sections, whereas SNAI3 immunostaining was performed  
224 on Bouin's fixed testis sections. Slides were dewaxed and rehydrated. Antigen retrieval was  
225 performed by heating slides for 10 mins in 10 mM citrate buffer (pH 6.0) using a 1000 W  
226 Pressure Cooker (Tefal). Slides were then treated with 0.3% hydrogen peroxide for 5 min at  
227 RT and washed 2 x 5 min at RT in tris-buffered saline (50 mM Tris, 150 mM NaCl, pH 7.5)  
228 (TBS). Blocking solution and antibody diluent consisted of 5% (v/v) normal serum diluted in  
229 TBS/0.1% BSA [(Sigma Aldrich, St Louis, USA) (to detect SNAI3)] or CAS block  
230 [(Invitrogen, Thermo Fisher Scientific, Waltham, USA) (to detect SNAI1 and SNAI2)] added  
231 for 1 hr at RT in a humid chamber. Sections were incubated overnight with primary antibody  
232 at RT in a humid chamber. Antibodies used to detect SNAI1 (GeneTex, GTX125918; 1:100),  
233 SNAI2 (abcam, ab27568, 1:100), SNAI3 (Santa Cruz Biotechnology, sc10439, 1:100), EED  
234 (R&D system, #AF5827, 1:200), EZH2 (Cell Signaling Technology, #5246, 1:200), LSD1  
235 (abcam, ab17721, 1:200). Anti-SNAI1, anti-SNAI2, anti-EZH2, and anti-LSD1 were detected  
236 using biotinylated anti-rabbit secondary antibody (Invitrogen, #656140, 1:500). SNAI3 was  
237 detected using biotinylated anti-goat secondary antibody (DAKO, #E0466, 1:500), whereas  
238 biotinylated anti-sheep secondary antibody was used for EED (Thermo Scientific, #618640,  
239 1:500). Signal was amplified with Vectastain Elite ABC kit reagents according to the  
240 manufacturer's instructions (Vector Laboratories, Burlingame, USA) followed by detection  
241 with DAB (3,3-diaminobenzidine tetrahydrochloride, DAKO, Steinheim, USA) to produce a  
242 brown precipitate. Sections were counterstained with Harris hematoxylin (Sigma Aldrich, St  
243 Louis, USA), dehydrated and mounted using DPX (Sigma Aldrich, St Louis, USA). Control  
244 sections were incubated in the absence of primary antibody to check for non-specific  
245 reactivity. Slides were imaged on a Zeiss imager A.1 microscope with an AxioCam MRc5.

246 The EED antibody used in this study was validated on *Eed* knockout samples (Prokopuk,  
247 Stringer et al. 2017). The specificity of EZH2 antibody is evident over 75 publications,

248 including the chromatin immunoprecipitation (ChIP) application (Snitow, Li et al. 2015). The  
249 specificity of LSD1 antibody is evident over 99 publications, including the ChIP application  
250 (Muralidharan, Khatri et al. 2017). The SNAI1 antibody was previously validated on *Snai1*  
251 knockout tissue (Horvay, Jarde et al. 2015). Western blots were performed in this study to  
252 validate the SNAI1, SNAI2 and SNAI3 antibodies using mouse testis lysates (see  
253 Supplementary Materials and Methods). The specificity of the SNAI2 antibody was further  
254 validated on *Snai2* knockout testis samples.

255

## 256 **Results**

### 257 **Snail mRNAs are expressed in distinct cell populations during postnatal testis** 258 **development**

259 To determine the pattern of Snail mRNA and protein expression through mouse testis  
260 development, we performed ddPCR and immunohistochemistry, respectively. *Snai1*, *Snai2*  
261 and *Snai3* transcripts were measured by ddPCR using RNA extracted from postnatal ages 7,  
262 14, 28 and adult (week 7) whole mouse testes. These ages correspond to germ cell population  
263 shifts that occur during the first postnatal wave of male germ cell development (Fig. 1 a). At  
264 day 7, the only cells present in the seminiferous tubule are undifferentiated and differentiated  
265 spermatogonia, and immature Sertoli cells. At day 14, spermatogonia and early  
266 spermatocytes are present, Sertoli cell proliferation has just arrested and tight junctions have  
267 begun to form between adjacent Sertoli cells to create the epithelial barrier required to  
268 support post-mitotic spermatogenesis. At day 28, spermatogonia, spermatocytes, round  
269 spermatids, and mature Sertoli cells are present. In the adult testis, all germ cell subtypes are  
270 present, including elongated spermatids, in addition to mature Sertoli cells. Droplet digital  
271 (dd) PCR revealed that all Snail family member genes were expressed at every postnatal age  
272 examined in the testis (Fig. 1 b-d). The *Snai1* transcript was detected at similar levels at each  
273 age (Fig. 1 b), suggesting that *Snai1* mRNA is present in multiple cell types within the testis.  
274 The *Snai2* transcript was most abundant at day 7, then significantly declined and was  
275 consistent through to adulthood (Fig. 1 c). The *Snai3* transcript was present at relatively low  
276 and consistent levels in all ages, but most abundant at day 7 (Fig. 1 d). This implies that  
277 *Snai2* and *Snai3* transcripts are enriched within the cells present prior the transition of mitotic  
278 to meiotic cells.

279

280 **Snail transcription factors display distinct mRNA profiles in the adult mouse testis and**  
281 **in isolated germ cells**

282 We next conducted a detailed analysis of Snail transcription factors in the adult mouse testis.  
283 This delineated the specific germ cell types in which Snail mRNAs are expressed, as the  
284 progression of germ cells between each differentiation state to form mature spermatozoa can  
285 be readily observed. To determine the cellular expression profiles of Snail transcripts, *in situ*  
286 hybridisation was performed on fixed wild-type adult mouse testis sections. *Snai1* was  
287 predominantly detected in spermatogonia and spermatocytes, with a faint signal apparent in  
288 round spermatids (Fig. 2 a, d). Similarly, the *Snai2* signal was strong in spermatogonia and  
289 spermatocytes, but not detectable in haploid germ cells (Fig. 2 b, e). *Snai3* showed a less  
290 restricted expression profile, with a signal evident in the cytoplasm of all germ cells and  
291 Sertoli cells (Fig. 2 c, f). *In situ* hybridisation results were verified by ddPCR which provided  
292 measurements of Snail transcript levels in isolated germ cells. Consistent with the *in situ*  
293 hybridisation data, *Snai1* and *Snai2* levels were higher in spermatogonia (Fig. 2 g) and  
294 spermatocytes (Fig. 2 j), but drastically lower in round spermatids (Fig. 2 k). In comparison,  
295 *Snai3* levels were highest in spermatogonia (Fig. 2 g), but significantly lower in  
296 spermatocytes and round spermatids (Fig. 2 j, k).

297

298 **Snail transcription factors display unique protein expression profiles during postnatal**  
299 **testis development**

300 To gain further understanding of the potential function of Snail transcription factors, we  
301 analysed Snail protein localisation in the postnatal mouse testis during the first wave of  
302 spermatogenesis. Germ and Sertoli cells were identified by their size, shape and chromatin  
303 morphology. SNAI1 displayed nuclear immunostaining in spermatogonia at day 10 (Fig. 3 a),  
304 in spermatogonia and spermatocytes at day 15 (Fig. 3 b) and in spermatogonia, spermatocytes  
305 and round spermatids at day 26 (Fig. 3 c). At postnatal days 10 and 15, SNAI2 was detected  
306 in the nucleus of spermatogonia, but was in the cytoplasm of spermatocytes at day 15 (Fig 3  
307 e). At day 26, SNAI2 was localised in the nucleus of spermatogonia, spermatocytes, round  
308 and elongated spermatids (Fig. 3 g), but in the adult mouse testis, SNAI2 appeared to be  
309 restricted in the nucleus of spermatogonia and spermatocytes, with a faint signal only in  
310 round spermatids (Fig. 3 h, Fig. S1). These data suggest that SNAI1 and SNAI2 are active  
311 during major cellular transitions. During the first wave of spermatogenesis, SNAI3

312 immunostaining was not detectable at day 10 (Fig. 3 i). A signal restricted to the Sertoli cell  
313 cytoplasm was observed at postnatal ages 15 (Fig. 3 j), 26 (Fig. 3 k), and in the adult (Fig. 3 l,  
314 Fig S2). However, the SNAI3 protein profile was different to that of its transcript, detected by  
315 *in situ* hybridisation in both germ and Sertoli cells in the adult mouse testis (Fig. 2 c, f). This  
316 suggests that there is tight regulation of SNAI3 transcript and protein synthesis.

317 Western blots were performed using lysates from adult mouse testis, isolated germ cells and  
318 whole mouse embryo (e11.5) to assess antibody specificity (Fig. S3). A single band at ~ 24  
319 kDa for SNAI1 was detected in 30 µg lysates from whole adult mouse testis and isolated  
320 germ cells. Additionally, two bands of expected sizes for SNAI3 were observed at ~ 45 and  
321 ~47 kDa in 30 µg lysates from whole embryo at e11.5 and adult mouse testis. SNAI2 could  
322 not be readily detected by Western blot. To determine specificity of antibody,  
323 immunohistochemistry was performed on adult testis from a *Snai2* knockout mouse (Fig. S3  
324 d). Compared to control, SNAI2 was absent from spermatogonia and spermatocytes. Non-  
325 specific signal was detected in the cytoplasm of elongated spermatids.

326 Overall these results demonstrate that the expression pattern of Snail transcription factors is  
327 dynamic, suggesting that each Snail family member has a unique role in the developing  
328 mouse testis.

329

### 330 **SNAI1 subcellular localisation in the adult mouse testis is Stage-specific**

331 Snail transcription factors are required to be nuclear in order to function. We investigated the  
332 subcellular localisation of SNAI1 in adult mouse testis by immunohistochemistry using an  
333 antibody that was previously used for detecting nuclear SNAI1 in intestinal cells (Horvay,  
334 Jarde et al. 2015). Interestingly, SNAI1 appeared to be nuclear in germ cells at specific  
335 Stages of the seminiferous epithelium cycle. At Stages I-VIII, strong signal was seen in the  
336 nucleus of spermatogonia, pachytene spermatocytes, and round spermatids (Fig. 4 a-c). At  
337 Stages IX-XII, some spermatogonia, pachytene and meiotically dividing spermatocytes  
338 displayed an intense nuclear staining; signal was absent from leptotene and zygotene  
339 spermatocytes (Fig. 4 d, e). The localisation of SNAI1 in elongated spermatids is particularly  
340 intriguing, as it changed. At Stages IX-XII, SNAI1 was in the nucleus of elongating  
341 spermatids (Fig. 4 d, e, g-j), but the signal became cytoplasmic at Stages I-VII (Fig. 4 a-c).  
342 This indicates that SNAI1 may have a specific role during the period of global transcriptional  
343 repression in elongating spermatids that occurs at Stages IX-XII.

344

345 **SNAI1 and SNAI2 share protein localisation patterns with co-repressors in the adult**  
346 **mouse testis.**

347 Snail family members need to recruit co-factors to mediate transcriptional repression. To  
348 understand the mechanism of Snail-mediated transcriptional regulation, we investigated the  
349 expression of EED and EZH2, PRC2 complex components, and LSD1 in the adult mouse  
350 testis, each of which is known to co-operate functionally with SNAI1 and SNAI2 (Mu,  
351 Starmer et al. 2014, Myrick, Christopher et al. 2017). By immunohistochemistry, EED and  
352 EZH2 displayed nuclear localisation in spermatogonia, leptotene, zygotenes, pachytene and  
353 meiotically dividing spermatocytes, and in Sertoli cells at Stages I-XII (Fig. 5). These  
354 proteins were detected in round spermatid nuclei at Stages I-VI (Fig. 5 a, b, f, g), while these  
355 signals were restricted to the cytoplasm of round spermatids at Stage VII-VIII (Fig. 5 c, h).

356 LSD1, lysine-specific histone demethylase 1, showed subcellular localisation profiles  
357 identical to SNAI1 in the adult mouse testis, with nuclear signal in spermatogonia,  
358 spermatocytes, round spermatids and Sertoli cells (Fig. 6). Like SNAI1, nuclear LSD1 was  
359 observed in elongated spermatids in a Stage-specific manner. At Stages IX-XII, LSD1 was  
360 nuclear in elongating spermatids (Fig. 6 d, e), but restricted to the cytoplasm of elongated  
361 spermatids following nuclear condensation at Stages I-VII (Fig. 6 a-c). Overall, these results  
362 identify potential partners required for Snail-mediated transcriptional regulation during  
363 spermatogenesis.

364

## 365 **Discussion**

366 Snail factors are of central importance to transcriptional regulation, cellular migration, signal  
367 transduction and chromatin remodelling in many developmental and disease systems, but  
368 their functional relevance to male fertility are poorly understood. As an initial approach to  
369 addressing this knowledge gap, we identified the cellular production sites of Snail  
370 transcription factors in the postnatal mouse testis. We show here for the first time that each  
371 Snail family members' transcript and protein has a distinct, developmentally regulated  
372 expression profile in cells of the postnatal mouse testis. This strongly suggests that each Snail  
373 family member has a distinct function during spermatogenesis.

374 SNAI1, SNAI2 and SNAI3 have similar molecular structures, however there are differences  
375 in their biological actions. SNAI1 functions as a potent survival factor (Vega, Morales et al.  
376 2004) and is essential to the preservation of stem cell function (Miller and Gauthier-Fisher  
377 2009) (Horvay, Jarde et al. 2015). Gene repression is best understood to be its mechanism of  
378 mediating these outcomes (De Craene, van Roy et al. 2005). In the testis, SNAI1 was  
379 previously suggested to be associated with spermatogonial stem cell maintenance; indirect  
380 upregulation of SNAI1 resulted in disruption of adherens junctions within the seminiferous  
381 epithelium and loss of spermatogonia (Kanarek, Horwitz et al. 2010). The present study  
382 describing SNAI1 mRNA and protein expression in the postnatal and adult mammalian testis  
383 provides new information that highlights the potential for SNAI1 to function at specific  
384 stages of spermatogenesis. Analyses by ddPCR and immunohistochemistry show that SNAI1  
385 mRNA and protein are present at every age in the postnatal testis (Fig. 1, Fig. 3).  
386 Intriguingly, SNAI1 protein is present in the nucleus of the most mature germ cell type  
387 present at each age, suggesting that SNAI1 is involved in the regulation of developmental  
388 switches during the cellular transitions of spermatogenesis. This function associated with  
389 SNAI1 is well-described during the epithelial to mesenchymal transition (EMT), in which  
390 nuclear-localised SNAI1 drives epithelial cells to acquire mesenchymal characteristics via the  
391 reprogramming of gene expression; key outcomes are cytoskeletal reorganisation and  
392 changes in cell behaviour (Wang, Shi et al. 2013). In the adult mouse testis (Fig. 2, Fig. 4), *in*  
393 *situ* hybridisation and ddPCR identify *Snail* predominantly in spermatocytes, although a less  
394 intense signal is also detected in spermatogonia and round spermatids. At a post-translational  
395 level, our analysis reveals a Stage- and cell-specific profile for SNAI1 protein in the adult  
396 mouse testis. SNAI1 is confined to the nucleus of a restricted number of spermatogonia, and  
397 of pachytene and diplotene spermatocytes, suggesting it could regulate gene transcription in  
398 both mitotic and meiotic germ cells. The two domains of Snail that are required for  
399 interaction with downstream targets and for recruitment of co-factors may be central to  
400 determining its diverse functions during spermatogenesis. In the post-meiotic phase, SNAI1  
401 localises within spermatid nuclei at Stages VIII-XII (Fig. 4), during the interval of extensive  
402 morphological changes that includes chromatin reorganisation and compaction. In the  
403 nucleus, histones are gradually replaced first by histone variants and transition proteins  
404 (Stages VIII-XII), then finally by protamines (Stages I-VII). As DNA is packaged,  
405 transcription is down-regulated (Hermo, Pelletier et al. 2010). Major contributors to  
406 transcriptional repression in spermatids are chromatin remodelling enzymes, capable of  
407 methylating or demethylating histones at specific residues (Rathke, Baarends et al. 2014).

408 Histone lysine demethylases 1 (LSD1) mediates transcriptional repression via demethylation  
409 of H3K4 (Gu and Lee 2013), and in the adult mouse testis LSD1 is observed in spermatid  
410 nuclei at Stages VIII-XII (Fig. 6). Consistent with the capacity of SNAI1 to recruit chromatin  
411 remodelling complexes at the SNAG domain, our results suggest that SNAI1 may interact  
412 with LSD1 to potentially mediate DNA packaging and promote repression of gene  
413 transcription.

414 Like SNAI1, SNAI2 regulates transcription and mediates the EMT (Villarejo, Cortes-Cabrera  
415 et al. 2014), however each induces common and distinct gene expression outcomes, as shown  
416 in epithelial cells (Moreno-Bueno, Cubillo et al. 2006). Specific SNAI2 functions in the testis  
417 are unknown, although it appears to be important for male fertility. Histological sections from  
418 *Snai2*-deficient mice were interpreted as displaying reduced germ and somatic Leydig cell  
419 numbers in the testis, though this outcome was not further quantified. This was hypothesised  
420 to arise from the disruption of the stem cell factor (SCF)/KIT signalling pathway, of known  
421 critical importance to spermatogonial cell migration, proliferation and differentiation. Droplet  
422 digital PCR indicates that the SNAI2 transcript and protein are present throughout postnatal  
423 testis development (Fig. 1, Fig. 3). In the adult testis, *in situ* hybridisation and ddPCR  
424 identified *Snai2* as more highly expressed in spermatocytes than in spermatogonia (Fig. 2).  
425 Consistent with the mRNA data, SNAI2 protein was detected in the nucleus of  
426 spermatogonia, and spermatocytes with a faint signal also observed in spermatids, thus  
427 SNAI2 may be involved in the events relating to mitotic and meiotic germ cell progression.  
428 Interestingly, EZH2 and EED, components of the PRC2 complex, co-localise with SNAI2 in  
429 nuclei of spermatogonia, spermatocytes and round spermatids (Fig. 5). Known for its unique  
430 roles in maintaining the undifferentiated spermatogonial pool through regulating SSC self-  
431 renewal, and in progression of meiosis (Mu, Starmer et al. 2014), the PRC2 complex  
432 represents a strong candidate to initiate SNAI2-mediate transcriptional repression. Because  
433 PRC2 controls many targets, it is not surprising that its spermatogenic phenotype, featuring  
434 the absence of post-meiotic cells, is more severe than that of *Snai2* knockout.

435

436 SNAI1 and SNAI2 are known to compensate for each other's loss by binding to the same  
437 target gene regulatory sequences (Chen and Gridley 2013). In the postnatal testis, we  
438 demonstrated that both SNAI1 and SNAI2 localise in the nucleus of spermatogonia and  
439 spermatocytes, where they may be functionally redundant. However SNAI3 displayed a

440 distinct expression profile. SNAI3 is structurally divergent and only recruits target genes with  
441 specific E-box sequences to its zinc finger domain. SNAI3 represses gene activity via its  
442 SNAG domain and an additional non-zinc finger region (Kataoka, Murayama et al. 2000).  
443 Although *Snai3* transcript is highly expressed in the skeletal muscle and thymus of adult  
444 wildtype mice (Kataoka, Murayama et al. 2000), its function is unknown. In this study, we  
445 demonstrate that *Snai3* is present at low levels at every age in the postnatal mouse testis (Fig.  
446 1), indicating that it is restricted to a selected population of cells. In the adult mouse testis, *in*  
447 *situ* hybridisation reveals that *Snai3* is expressed in Sertoli and all germ cells (Fig. 2). The  
448 *Snai3* expression profile in germ cells was confirmed by ddPCR, with *Snai3* levels higher in  
449 spermatogonia and spermatocytes, but lower in round spermatids (Fig. 2). In the developing  
450 postnatal testis, SNAI3 protein was visible in the Sertoli cell cytoplasm from 15 dpp, but not  
451 earlier, until adulthood (Fig. 3), indicating that SNAI3 might have a specific role during the  
452 formation of Sertoli-germ cell adherens junctions, Sertoli-Sertoli tight junctions, which  
453 contribute to the blood-testis barrier. It is intriguing that the major components of the  
454 adherens and tight junctions are E-Cadherin (Tanwar, Zhang et al. 2011), occludins and  
455 claudins, essential for blood-testis barrier integrity (Morrow, Mruk et al. 2010) and well-  
456 known Snail downstream targets (Nieto 2002, Ikenouchi, Matsuda et al. 2003). The absence  
457 of a SNAI3 protein signal in any germ cells may reflect a high turnover or lack of synthesis in  
458 the spermatogenic lineage. To our knowledge, there is no evidence for alternative isoforms.

459

460 In summary, this study has provided evidence that synthesis of each of the three mammalian  
461 Snail transcription factor is tightly regulated during mouse spermatogenesis. The cellular  
462 distribution of Snail transcripts and proteins in the postnatal mouse testis indicates their likely  
463 sites of function, including in relationship to the regulatory mechanisms that mediate  
464 developmental changes during cellular transitions in spermatogenesis and during Sertoli cell  
465 development. These data provide a foundation for defining what regulates Snail levels and  
466 target genes, many of which are implicated in key processes in other biological systems.

467

468 **Acknowledgments:** The authors would like to thank Reyhan Akhtar, Dr Katja Horvay and  
469 Franca Casagrande for assistance with Droplet digital PCR. The authors acknowledge  
470 Elizabeth Richards and Penny Whiley for technical support. We also like to thank Dr Patrick

471 Western and Dr Jody Haigh for providing aliquots of the EED and EZH2, and LSD1  
472 antibodies, respectively.

473 **Author Contributions:** DJM, KLL, HEA, GRH designed experiments, interpreted data and  
474 wrote the manuscript. DJM performed experiments. EAM provided materials for the study.

475 **Compliance with ethical standards**

476 **Conflict of interest:** The authors have no conflicts of interest in presenting information and  
477 material described in this paper.

478

479

## 480 **References**

481 Ahmed, E. A. and D. G. de Rooij (2009). "Staging of mouse seminiferous tubule cross-sections."  
482 *Methods Mol Biol* **558**: 263-277.

483

484 Alberga, A., J. L. Boulay, E. Kempe, C. Dennefeld and M. Haenlin (1991). "The snail gene required for  
485 mesoderm formation in *Drosophila* is expressed dynamically in derivatives of all three germ layers."  
486 *Development* **111**(4): 983-992.

487

488 Batlle, E., E. Sancho, C. Franci, D. Dominguez, M. Monfar, J. Baulida and A. Garcia De Herreros  
489 (2000). "The transcription factor snail is a repressor of E-cadherin gene expression in epithelial  
490 tumour cells." *Nat Cell Biol* **2**(2): 84-89.

491

492 Bradley, C. K., C. R. Norton, Y. Chen, X. Han, C. J. Booth, J. K. Yoon, L. T. Krebs and T. Gridley (2013).  
493 "The snail family gene *snai3* is not essential for embryogenesis in mice." *PLoS One* **8**(6): e65344.

494

495 Bromfield, E. G., R. J. Aitken, E. A. McLaughlin and B. Nixon (2017). "Proteolytic degradation of heat  
496 shock protein A2 occurs in response to oxidative stress in male germ cells of the mouse." *Mol Hum  
497 Reprod* **23**(2): 91-105.

498

499 Chen, Y. and T. Gridley (2013). "Compensatory regulation of the *Snai1* and *Snai2* genes during  
500 chondrogenesis." *J Bone Miner Res* **28**(6): 1412-1421.

501

502 Chiang, C. and K. Ayyanathan (2013). "Snail/Gfi-1 (SNAG) family zinc finger proteins in transcription  
503 regulation, chromatin dynamics, cell signaling, development, and disease." *Cytokine Growth Factor*  
504 *Rev* **24**(2): 123-131.

505

506 Cobaleda, C., M. Perez-Caro, C. Vicente-Duenas and I. Sanchez-Garcia (2007). "Function of the zinc-  
507 finger transcription factor SNAI2 in cancer and development." *Annu Rev Genet* **41**: 41-61.

508

509 De Craene, B., F. van Roy and G. Berx (2005). "Unraveling signalling cascades for the Snail family of  
510 transcription factors." *Cell Signal* **17**(5): 535-547.

511

512 Dias, V. L., E. Rajpert-De Meyts, R. McLachlan and K. L. Loveland (2009). "Analysis of activin/TGFB-  
513 signaling modulators within the normal and dysfunctional adult human testis reveals evidence of  
514 altered signaling capacity in a subset of seminomas." *Reproduction* **138**(5): 801-811.

515

516 Eddy, E. M. (1998). "Regulation of gene expression during spermatogenesis." *Semin Cell Dev Biol*  
517 **9**(4): 451-457.

518

519 Gu, B. and M. G. Lee (2013). "Histone H3 lysine 4 methyltransferases and demethylases in self-  
520 renewal and differentiation of stem cells." *Cell Biosci* **3**(1): 39.

521

522 Hermo, L., R. M. Pelletier, D. G. Cyr and C. E. Smith (2010). "Surfing the wave, cycle, life history, and  
523 genes/proteins expressed by testicular germ cells. Part 2: changes in spermatid organelles associated  
524 with development of spermatozoa." *Microsc Res Tech* **73**(4): 279-319.

525

526 Hess, R. A. and L. Renato de Franca (2008). "Spermatogenesis and cycle of the seminiferous  
527 epithelium." *Adv Exp Med Biol* **636**: 1-15.

528 Horvay, K., T. Jarde, F. Casagrande, V. M. Perreau, K. Haigh, C. M. Nefzger, R. Akhtar, T. Gridley, G.  
529 Berx, J. J. Haigh, N. Barker, J. M. Polo, G. R. Hime and H. E. Abud (2015). "Snai1 regulates cell lineage  
530 allocation and stem cell maintenance in the mouse intestinal epithelium." *EMBO J* **34**(10): 1319-  
531 1335.

532

533 Ikenouchi, J., M. Matsuda, M. Furuse and S. Tsukita (2003). "Regulation of tight junctions during the  
534 epithelium-mesenchyme transition: direct repression of the gene expression of claudins/occludin by  
535 Snail." *J Cell Sci* **116**(Pt 10): 1959-1967.

536

537 Itman, C., C. Wong, P. A. Whiley, D. Fernando and K. L. Loveland (2011). "TGFbeta superfamily  
538 signaling regulators are differentially expressed in the developing and adult mouse testis."  
539 *Spermatogenesis* **1**(1): 63-72.

540

541 Jiang, R., Y. Lan, C. R. Norton, J. P. Sundberg and T. Gridley (1998). "The Slug gene is not essential for  
542 mesoderm or neural crest development in mice." *Dev Biol* **198**(2): 277-285.

543

544 Kalluri, R. and R. A. Weinberg (2009). "The basics of epithelial-mesenchymal transition." *J Clin Invest*  
545 **119**(6): 1420-1428.

546

547 Kanarek, N., E. Horwitz, I. Mayan, M. Leshets, G. Cojocaru, M. Davis, B. Z. Tsuberi, E. Pikarsky, M.  
548 Pagano and Y. Ben-Neriah (2010). "Spermatogenesis rescue in a mouse deficient for the ubiquitin  
549 ligase SCF{beta}-TrCP by single substrate depletion." *Genes Dev* **24**(5): 470-477.

550

551 Kataoka, H., T. Murayama, M. Yokode, S. Mori, H. Sano, H. Ozaki, Y. Yokota, S. Nishikawa and T. Kita  
552 (2000). "A novel snail-related transcription factor Smuc regulates basic helix-loop-helix transcription  
553 factor activities via specific E-box motifs." *Nucleic Acids Res* **28**(2): 626-633.

554

555 Kramer, J. M. and R. P. Erickson (1981). "Developmental program of PGK-1 and PGK-2 isozymes in  
556 spermatogenic cells of the mouse: specific activities and rates of synthesis." *Dev Biol* **87**(1): 37-45.

557

558 Leblond, C. P. and Y. Clermont (1952). "Definition of the stages of the cycle of the seminiferous  
559 epithelium in the rat." *Ann N Y Acad Sci* **55**(4): 548-573.

560

561 Lin, Y., C. Dong and B. P. Zhou (2014). "Epigenetic regulation of EMT: the Snail story." *Curr Pharm*  
562 *Des* **20**(11): 1698-1705.

563

564 McIver, S. C., S. J. Stanger, D. M. Santarelli, S. D. Roman, B. Nixon and E. A. McLaughlin (2012). "A  
565 unique combination of male germ cell miRNAs coordinates gonocyte differentiation." *PLoS One* **7**(4):  
566 e35553.

567

568 Miller, F. D. and A. Gauthier-Fisher (2009). "Home at last: neural stem cell niches defined." *Cell Stem*  
569 *Cell* **4**(6): 507-510.

570

571 Moreno-Bueno, G., E. Cubillo, D. Sarrio, H. Peinado, S. M. Rodriguez-Pinilla, S. Villa, V. Bolos, M.  
572 Jorda, A. Fabra, F. Portillo, J. Palacios and A. Cano (2006). "Genetic profiling of epithelial cells  
573 expressing E-cadherin repressors reveals a distinct role for Snail, Slug, and E47 factors in epithelial-  
574 mesenchymal transition." *Cancer Res* **66**(19): 9543-9556.

575

576 Morrow, C. M., D. Mruk, C. Y. Cheng and R. A. Hess (2010). "Claudin and occludin expression and  
577 function in the seminiferous epithelium." *Philos Trans R Soc Lond B Biol Sci* **365**(1546): 1679-1696.

578

579 Mu, W., J. Starmer, A. M. Fedoriw, D. Yee and T. Magnuson (2014). "Repression of the soma-specific  
580 transcriptome by Polycomb-repressive complex 2 promotes male germ cell development." *Genes  
581 Dev* **28**(18): 2056-2069.

582

583 Muralidharan, B., Z. Khatri, U. Maheshwari, R. Gupta, B. Roy, S. J. Pradhan, K. Karmodiya, H.  
584 Padmanabhan, A. S. Shetty, C. Balaji, U. Kolthur-Seetharam, J. D. Macklis, S. Galande and S. Tole  
585 (2017). "LHX2 Interacts with the NuRD Complex and Regulates Cortical Neuron Subtype  
586 Determinants Fezf2 and Sox11." *J Neurosci* **37**(1): 194-203.

587

588 Myrick, D. A., M. A. Christopher, A. M. Scott, A. K. Simon, P. G. Donlin-Asp, W. G. Kelly and D. J. Katz  
589 (2017). "KDM1A/LSD1 regulates the differentiation and maintenance of spermatogonia in mice."  
590 *PLoS One* **12**(5): e0177473.

591

592 Nieto, M. A. (2002). "The snail superfamily of zinc-finger transcription factors." *Nat Rev Mol Cell Biol*  
593 **3**(3): 155-166.

594

595 Oakberg, E. F. (1956). "Duration of spermatogenesis in the mouse and timing of stages of the cycle of  
596 the seminiferous epithelium." *Am J Anat* **99**(3): 507-516.

597

598 Perez-Losada, J., M. Sanchez-Martin, A. Rodriguez-Garcia, M. L. Sanchez, A. Orfao, T. Flores and I.  
599 Sanchez-Garcia (2002). "Zinc-finger transcription factor Slug contributes to the function of the stem  
600 cell factor c-kit signaling pathway." *Blood* **100**(4): 1274-1286.

601

602 Pioli, P. D., T. J. Dahlem, J. J. Weis and J. H. Weis (2013). "Deletion of Snai2 and Snai3 results in  
603 impaired physical development compounded by lymphocyte deficiency." *PLoS One* **8**(7): e69216.

604

605 Prokopuk, L., J. M. Stringer, K. Hogg, K. D. Elgass and P. S. Western (2017). "PRC2 is required for  
606 extensive reorganization of H3K27me3 during epigenetic reprogramming in mouse fetal germ cells."  
607 *Epigenetics Chromatin* **10**: 7.

608

609 Rathke, C., W. M. Baarends, S. Awe and R. Renkawitz-Pohl (2014). "Chromatin dynamics during  
610 spermiogenesis." *Biochim Biophys Acta* **1839**(3): 155-168.

611

612 Shalet, S. M. (2009). "Normal testicular function and spermatogenesis." *Pediatr Blood Cancer* **53**(2):  
613 285-288.

614

615 Snitow, M. E., S. Li, M. P. Morley, K. Rathi, M. M. Lu, R. S. Kadzik, K. M. Stewart and E. E. Morrisey  
616 (2015). "Ezh2 represses the basal cell lineage during lung endoderm development." *Development*  
617 **142**(1): 108-117.

618

619 Tanwar, P. S., L. Zhang and J. M. Teixeira (2011). "Adenomatous polyposis coli (APC) is essential for  
620 maintaining the integrity of the seminiferous epithelium." *Mol Endocrinol* **25**(10): 1725-1739.

621

622 Turner, F. E., S. Broad, F. L. Khanim, A. Jeanes, S. Talma, S. Hughes, C. Tselepis and N. A. Hotchin  
623 (2006). "Slug regulates integrin expression and cell proliferation in human epidermal keratinocytes."  
624 *J Biol Chem* **281**(30): 21321-21331.

625

626 Uygur, B. and W. S. Wu (2011). "SLUG promotes prostate cancer cell migration and invasion via  
627 CXCR4/CXCL12 axis." *Mol Cancer* **10**: 139.

628

629 Vega, S., A. V. Morales, O. H. Ocana, F. Valdes, I. Fabregat and M. A. Nieto (2004). "Snail blocks the  
630 cell cycle and confers resistance to cell death." *Genes Dev* **18**(10): 1131-1143.

631

632 Villarejo, A., A. Cortes-Cabrera, P. Molina-Ortiz, F. Portillo and A. Cano (2014). "Differential role of  
633 Snail1 and Snail2 zinc fingers in E-cadherin repression and epithelial to mesenchymal transition." *J*  
634 *Biol Chem* **289**(2): 930-941.

635

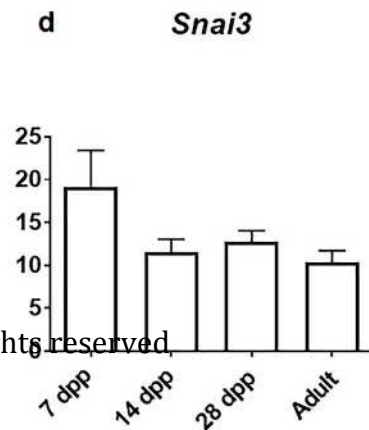
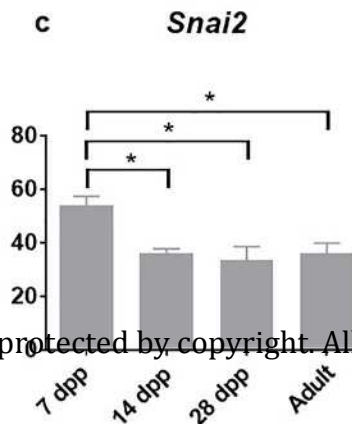
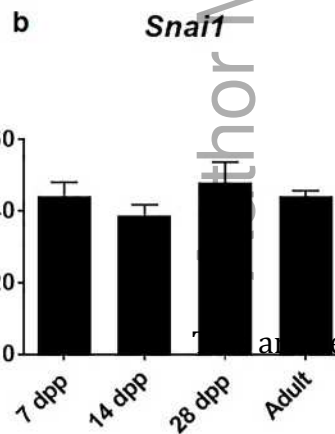
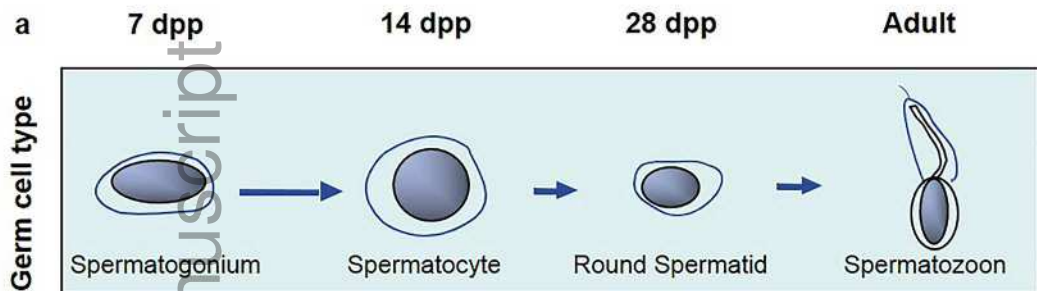
636 Wang, Y., J. Shi, K. Chai, X. Ying and B. P. Zhou (2013). "The Role of Snail in EMT and Tumorigenesis."  
637 *Curr Cancer Drug Targets* **13**(9): 963-972.

# Author Manuscript

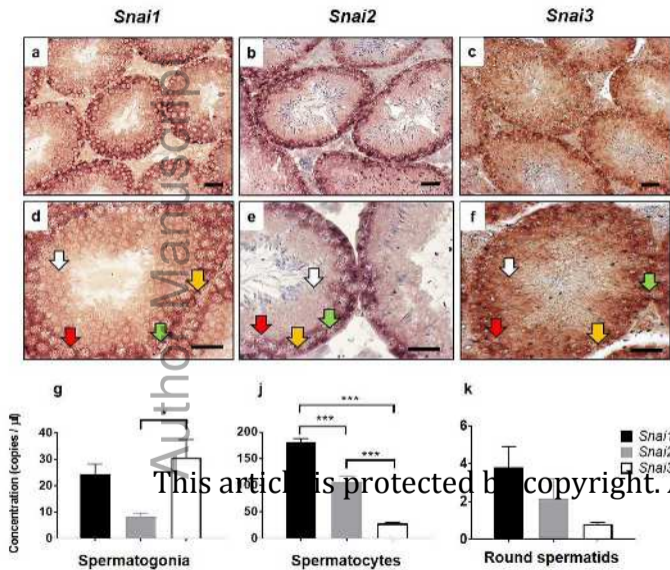
<b>Gene</b>	<b>Accession number</b>	<b>Forward (5'-3')</b>	<b>Reverse (5'-3')</b>	<b>Region amplified</b>
Snai1	NM_011427.3	TTCAGGCCACCTTCTTTGAG	TGAAACAGGTGTCACCAGGA	1178-1353
Snai2	NM_011415.2	TGATGCCTGGTTGTCATCAG	GACACGCACCAGGAATGTTT	1462-1666
Snai3	NM_013914.2	TCTGCTGGACCTGTTCCAAA	GGGGCAGGAGAAAATGTGTC	1159- 1373

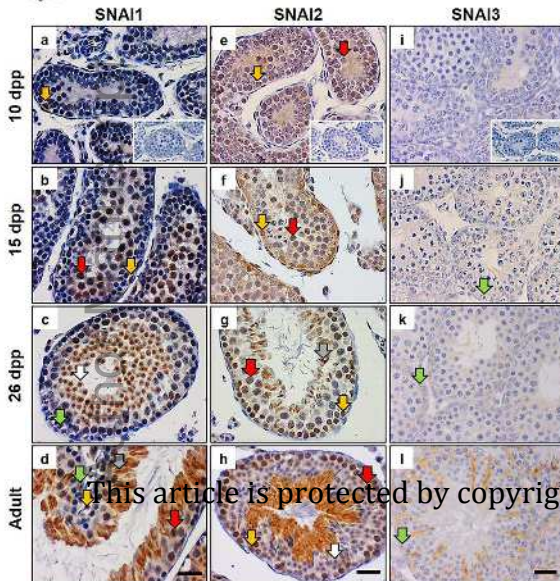
**Table 1. Primer sequences used for generation of in situ hybridisation probes to detect mouse transcripts.**

Fig. 1

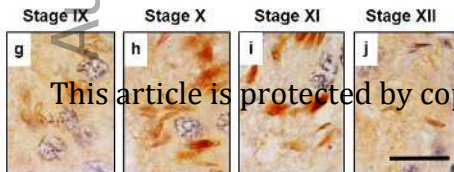
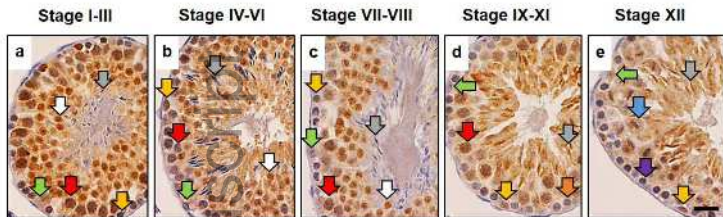


bioRxiv preprint doi: <https://doi.org/10.1101/124651>; this version posted July 11, 2017. The copyright holder for this preprint (which was not certified by peer review) is the author/funder, who has granted bioRxiv a license to display the preprint in perpetuity. It is made available under aCC-BY-NC-ND 4.0 International license.



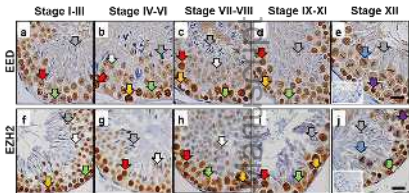


This article is protected by copyright. All rights reserved.



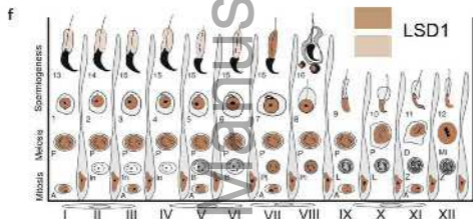
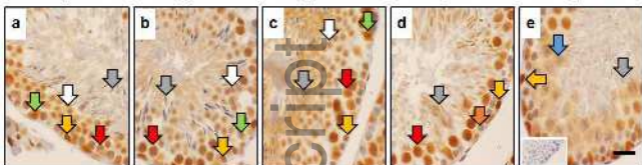
This article is protected by copyright. All rights reserved.

## andr\_12465\_f5.pdf



This article is

Stage I-III      Stage IV-VI      Stage VII-VIII      Stage IX-XI      Stage XII

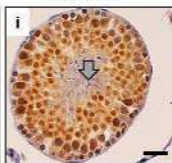
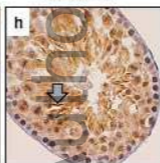
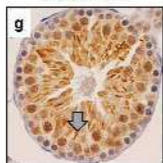


Stage IX-XI

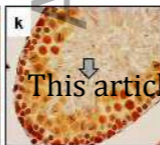
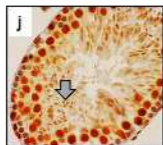
Stage XII

Stage I-III

SNAI1



LSD1



This article is protected by copyright